Applied Geography 90 (2018) 239–247

Contents lists available at ScienceDirect

Applied Geography

journal homepage: www.elsevier.com/locate/apgeog

Modeling population density based on nighttime light images and land use data in China

Minghong Tan[a,b,*], Xiubin Li[a,c], Shiji Li[a,c], Liangjie Xin[a], Xue Wang[a], Qian Li[d], Wei Li[a,c], Yuanyuan Li[a,c], Wenli Xiang[a,c]

[a] Key Laboratory of Land Surface Pattern and Simulation, Institute of Geographic Sciences and Natural Resources Research (IGSNRR), Chinese Academy of Sciences (CAS), Beijing, 100101, China
[b] International College, University of Chinese Academy of Sciences, Beijing, 100190, China
[c] College of Resources and Environment, University of Chinese Academy of Sciences, Beijing, 100190, China
[d] Business School, Shandong University, Weihai, 264209, China

ARTICLE INFO

Keywords:
Nighttime light images
Census data
Land use
Population density simulation
China

ABSTRACT

Population change is a key variable that influences climate change, ecological construction, soil and water use, and economic growth. Census data are always point data, whereas planar data are often required in scientific research. By using nighttime light (NTL) images and land use data, combined with the fifth and sixth census data of China at the county level, we carried out spatial matching on the population of each county, respectively, and established population density diagrams of China for 2000 and 2010, which had a spatial resolution of 1 × 1 km. The method proposed in this paper is relatively simple and has a high simulation precision. The results showed that during the first ten years of the 21st century, there are some remarkable characteristics in Chinese population spatial pattern change: 1) the "disappearance" of intermediate-density regions; namely, areas with a population density between 500 and 1500 persons/km^2 have decreased by 41% during the ten years; 2) continuous growth of high-density regions; namely, areas with a population density of more than 1500 persons/km^2 have increased by 76%; 3) an expansion tendency of low-density regions similar to high-density regions.

Since China's reform and opening up, the country has been entering into a rapid urbanization phase and experienced the largest rural-urban population migration in human history (Zhang & Song, 2003). From 1990 to 2010, the urban population increased from 302 to 671 million; at the same time, the rural population decreased from 841 to 670 million (NBSC, 2013). Urban-rural population migration has greatly changed the production and life styles of humans and exerts a significant impact on the natural environment and the social economy.

Until now, China has carried out six censuses, which provide a solid data foundation to comprehend China's population status and the relationship between humans and their natural environment (Li, Sun, Tan, & Li, 2016). However, census data are usually obtained based on administrative units; however, administrative units at the same hierarchy of China usually show significant differences in their administrative areas in different regions. For instance, some counties have an administrative area of less than 100 km^2, while others have a large area (e.g., the area of Ruoqiang County in Xinjiang covers 202,000 km^2). Moreover, even in the same county, due to differences in geographical environment and economic development level, population distribution is also very imbalanced. In addition, most studies do not use the administrative unit as the research object (Ryan et al., 2017; Tan et al., 2008; Tritsch & Le Tourneau, 2016; Yang, Jiang, Luo, & Zheng, 2012), but rather consider the basin or geographic unit. Therefore, previous studies conducted spatial simulation on the population distribution using different methods (Anderson, Tuttle, Powell, & Sutton, 2010; Bagan & Yamagata, 2015; Liu et al., 2003b; Lung, Lübker, Ngochoch, & Schaab, 2013; Tian, Yue, Zhu, & Clinton, 2005). For example, Liu et al. (2003b) simulated China's population density by combining digital elevation data, net primary productivity data, transportation infrastructure data, and urban scale data, based on the gravity model method.

Nighttime light data from Defense Meteorological Satellite Program's Operational Linescan System (DMSP/OLS) are important indicators that reflect human agglomeration and energy consumption, which provide a stable and persistent data source (Elvidge et al., 2001; Hsu, Baugh, Ghosh, Zhizhin, & Elvidge, 2015). Currently, these data are widely used to evaluate urban growth (Imhoff, Lawrence, Stutter, & Elvidget, 1997; Lu, Tian, Zhou, & Ge, 2008; Ma, Zhou, Zhou, Haynie,

* Corresponding author. Key Laboratory of Land Surface Pattern and Simulation, Institute of Geographic Sciences and Natural Resources Research, Chinese Academy of Sciences, Beijing, 100101, China.
E-mail address: tanmh@igsnrr.ac.cn (M. Tan).

https://doi.org/10.1016/j.apgeog.2017.12.012
Received 2 January 2017; Received in revised form 13 December 2017; Accepted 13 December 2017
Available online 27 December 2017
0143-6228/ © 2017 Elsevier Ltd. All rights reserved.

Table 1
Comparison of previous studies related to population density simulation in China.

Authors	Models	Data used	Simulated year	Data format of density simulation
Wang, Feng, Yang, and You (2014)		Census, land area at the county level	2000, 2010	Average density at the county level
Tian et al. (2005)	Regression method, buffer analysis et al.	Population, road, railway, river, city distribution, rural population, urban population, land use map	2000	Grid
Liu et al. (2003b)	Gravity model	Data of climate, soil, remote sensing, way, railway, elevation et al.	2000	Grid
Zhuo et al. (2005)	Regression and allometric models	NTL images, NDVI, non-agricultural population, population	1998	Grid
Lo (2001)	Regression method	NTL images, non-agricultural population, rural population	1997	Average density at the county level
Zeng et al. (2011)	Regression method	NTL intensity, land use	2000	Grid
Dobson, Brlght, Coleman, Durfee, and Worley (2000)	Gravity model et al.	Road proximity, slope, land cover, and nighttime lights.	1998	Grid

Pei, & Xu, 2015; Pandey, Joshi, & Seto, 2013; Shao & Liu, 2014; Small, Pozzi, & Elvidge, 2005; Su et al., 2015; Wei, Liu, Song, Yu, & Xiu, 2014; Xiao, Wang, Feng, Zhang, & Yang, 2014; Yi et al., 2014; Yue, Zhang, & Liu, 2016; Zhang & Su, 2016; Zhou et al., 2014), economic development (Chen & Nordhausa, 2011; Elvidge et al., 2009; Keola, Andersson, & Hall, 2015; Levin & Duke, 2012; Propastin & Kappas, 2012; Wu, Wang, Li, & Peng, 2013), and urban transition (Saksena et al., 2014; Tan, 2015). Some scholars have analyzed the relationship between population distribution and light intensity in different regions, showing a significant correlation between them (Anderson et al., 2010; Bagan & Yamagata, 2015). In addition, some authors have conducted spatial matching on the demographic data by using light image data (Amaral, Câmara, Monteiro, Quintanilha, & Elvidge, 2005; Sutton, 1997). For example, Zhuo et al. (2005) conducted simulation on the population distribution of China in 1998 by using vegetation coverage data, light image data, and non-agricultural population and rural population data, and obtained good simulation results.

To sum up, the existing researches related to population density simulation are relatively complex and involve various and abundant data sets (Table 1). These complex simulation processes may reduce the spatial matching accuracy of population distribution. In addition, such studies usually divide a country into several areas (Zeng, Zhou, Wang, Yan, & Zhao, 2011) to establish the relationship between population density and light intensity, and then conduct spatial simulation on the population density at the regional scale. Furthermore, until now, the spatial simulation has been ignored based on the fifth (2000) and sixth census (2010) data of China, using the same method, and comparison of spatial changes in population density is also not enough, especially at the grid level across the country.

In this paper, we used a simpler and more direct simulation model to conduct spatial matching and simulation on the demographic data for each county in China, respectively. Specifically, based on the fifth and sixth census data, light image and land use data, we analyzed the relationships between population density and light intensity, cultivated land distribution, and settlement distribution at the county level after removing unused land and water areas (Fig. 1). On the basis of these relationships, we conducted spatial matching on the demographic data of each county, respectively, and obtained spatial distribution diagrams (with a resolution of 1 × 1 km) of population density in 2000 and 2010, which were then used to analyze the variation of population density. The simulated population density data can be used as the input data to explore the influences of population changes on the natural environment, ecological footprint, and climate change.

1. Data sources

Land use data in 2000 were obtained from the land use database with a scale of 1:100,000, provided by the Resources and Environment Data Center, CAS. The data were manually interpreted mainly based on the Landsat TM data. A large amount of field investigation proved that land use classification had an accuracy of more than 90% (Liu, Liu, Deng, Zhuang, & Zhang, 2002, 2003a).

Nighttime light data were obtained from the time series data of DMSP/OLS (http://www.ngdc.noaa.gov/eog/dmsp/downloadV4composites.html accessed October 15, 2014). The NTL images used in this study in 2000 and 2010 were obtained from satellites F14 and F18, respectively. The data were in the grid format, with grid values between 0 and 63 (Keola et al., 2015), in which the larger values represent higher light intensity. Across China, the grid values varied between 1 and 63. Since the light image data were obtained from different satellites, in order to conduct comparisons for time series data, it is necessary to calibrate these data to endow the light image data in different years with comparability. In this study, on the basis of respectively simulating the relationships among light image intensity (DN value), residential land proportion, and population density in 2000 and 2010, we carried out spatial matching on the census data. Since time series comparison for the light image intensity was not conducted here, we did not calibrate the light image data in different years.

Demographic data in 2000 and 2010 were obtained from the database of the fifth and sixth census at the county level. Demographic data in the 2005 were from China County Statistical Yearbook in 2006 (NBSC, 2006). The demographic data used in this study were the data of permanent population defined by the census (NBSC, 2002; 2012). According to the definition, migrants were recorded at their current abode rather than at their place of registration if they lived at the abode for over 6 months/year. These migrants are regarded as permanent population.

2. Methods

According to China's land use map of the year 2000, water areas and unused land were removed as uninhabited areas and the population density values of these regions were set as 0. In this study, we firstly analyzed the relationships between the light images, cultivated land distribution, settlement distribution, and the population density at the county level. Subsequently, we conducted spatial matching and simulation on the census data at the county level. Finally, the simulation results were verified by the township-level census data.

As previously introduced, light images are closely related to human activities, which can reflect the population density to a large extent. Therefore, the premise of model simulation is to determine the quantitative relation between light image intensity and population density. Due to the lack of demographic data, it is extremely difficult to describe the quantitative relationship at the grid level. Tian et al. (2005) analyzed the relationship between the population and different land use

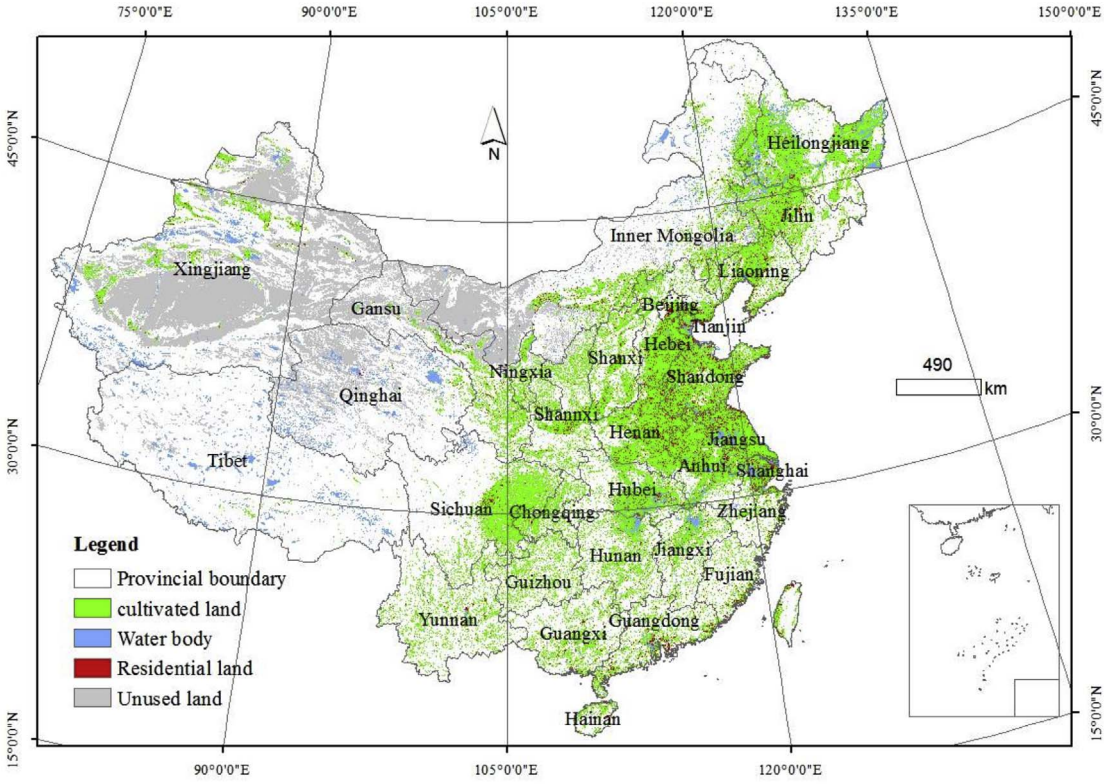

Fig. 1. Land use type distribution of China in 2000. Note: Data were obtained from the Resources and Environment Data Center, CAS.

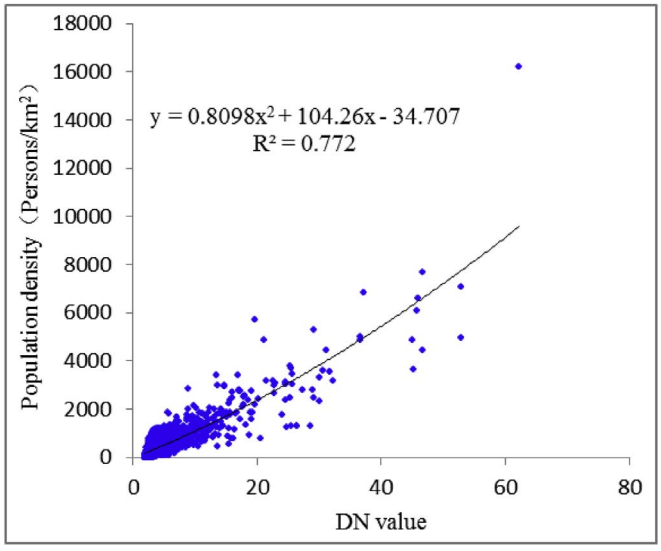

Fig. 2. Relationship between light intensity and population density at the county level in 2000. Note: light intensity and population density were calculated using Eqs. (1) and (2), respectively.

types at the county level in China; on this basis, they conducted spatial matching on the population at the grid level. In a similar way, we firstly quantitatively analyzed the relationships between population density, light intensity and the land use types of 2300 districts/counties of China. These quantitative relationships were then viewed as the basis of conducting spatial matching on demographic data in order to simulate population spatial distribution of each county, respectively. Because the spatial resolution of light image data was 1 × 1 km and that of land use data was 30 × 30 m, we used the proportions of different land use types in each grid of light image data as the land use variables and incorporated them into the model. In the simulation process, we found that when we simulated the population density using the multiple regression model, some variables, such as the proportions of forest land and grass land, had negative effects on the independent variables (i.e., population density), which led to negative values of population density. Moreover, the model validation results also showed that the introduction of the two variables, i.e., forest land distribution and grass land distribution, had no significant effects on the simulation accuracy. Hence, we only adopted two variables that were related to land use types, i.e., residential land proportion and cultivated land proportion, to carry out the simulation. The specific simulation process is as follows:

On the basis of removing the unused land and water bodies, the average DN value of nighttime light of county i (x_i) can be calculated as:

$$x_i = \frac{\sum_{j=1}^{N} (DN)_{ij}}{N_i} \quad (1)$$

where $(DN)_{ij}$ and N_i are the DN value of grid j of county i and the total grid number of this county, respectively. Similarly, on the basis of removing the unused land and water bodies, the population density y_i of county i can be calculated as:

$$y_i = Pop_i / S_i \quad (2)$$

where Pop_i and S_i are the population and area (km^2) of county i. Figs. 2 and 3 show the relationships between population density and light image at the county level. The results showed that with the increase of light intensity, the population density showed a trend of rapid growth. This trend can be described by the right branch of the parabola, which offered the best performance after making a comparison with other models including linear, exponential, and logarithmic models. Similarly, at the county level, the relationship between the proportion of residential land and the population density also presented a parabolic relationship. Like the existing literature, we simulated the relationship between the independent variables and population density using the multiple regression model. However, using this model, it should be

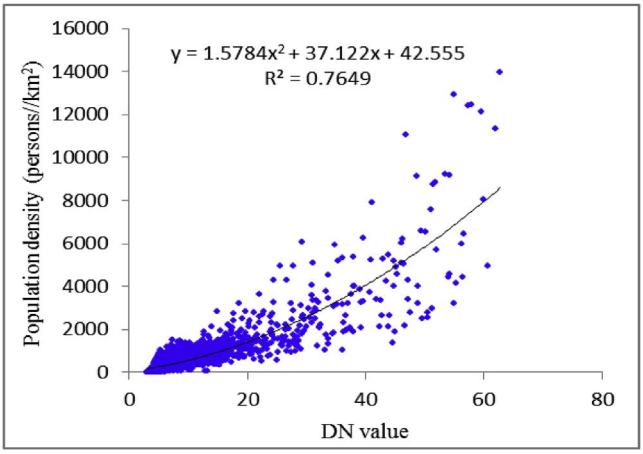

Fig. 3. Relationship between light intensity and population density at the county level in 2010. Note: light intensity and population density were calculated using Eqs. (1) and (2), respectively.

ensured that the relationship between independent and dependent variable is linear. To this end, we used the square root of the population density as the dependent variable. Thus, the simulation equations in 2000 and 2010 are as follows:

$$\sqrt{y_{2000i}} = 11.387 \times DN_{2000i} + 1.066 \times Ara_{2000i} + 44.784 \times Sett_{2000i} + 3.485 \quad (3)$$

$$\sqrt{y_{2010i}} = 7.259 \times DN_{2010i} + 0.774 \times Ara_{2010i} + 58.595 \times Sett_{2010i} + 4.946 \quad (4)$$

In Eq. (3), $\sqrt{y_{2000i}}$, DN_{2000i}, Ara_{2000i}, and $Sett_{2000i}$ represent the square root of population density, the average value of DN, cultivated land proportion, and residential land proportion of county i in 2000, respectively; after substituting the counterpart values in 2010 into Eq. (3), Eq. (4) can be obtained. In the regression models of 2000 and 2010, the adjusted R^2 values are 0.794 and 0.804, respectively.

Based on the above method, the population density (y_{ij}) of grid j in County i in 2000 and 2010 can be calculated according to the simulation equations for 2000 and 2010, respectively. However, in some counties, the calculated total population may be higher or lower than the corresponding census values. To this end, the calculated total population should be further calibrated by the census data to obtain the population density value of each grid for each county:

$$\rho_{ij} = Pop_i \times \frac{y_{ij}}{\sum_{j=1}^{N} y_{ij}} \quad (5)$$

where ρ_{ij} is the calibrated population density of grid j in county i.

In non-census years, it is very difficult to obtain spatial distribution of population. Based on the results of this study, we designed a method to project spatial distribution map of population. According to Eqs. (3) and (4), we know that population density at the raster level can be projected using a similar method in 2000 and 2010. Thus, based on the consumption that population of each raster changed linearly from 2000 to 2010, we can know that if a year is closer to a census year, its spatial distribution has a more similar feature to the census year. For instance, spatial distribution of population in 2001 was more similar to that in 2000, while the distribution in 2009 was more similar to 2010. Thus, we can project spatial distribution of non-census years between 2000 and 2010, using the following equation:

$$\rho_{ij}^{k} = \frac{(2010 - k) \times \rho_{ij}^{2000} + (k - 2000) \times \rho_{ij}^{2010}}{2010 - 2000} \quad (6)$$

where ρ_{ij}^{k} is the population density of grid j of county i in year k. Here, the values of k are between 2000 and 2010.

Finally, to verify the precision of the simulation results of the census years, this study evaluated the simulation results obtained by the use of census data of villages and towns (sub-districts). For the non-census years, we tested the simulation results at the county level, considering

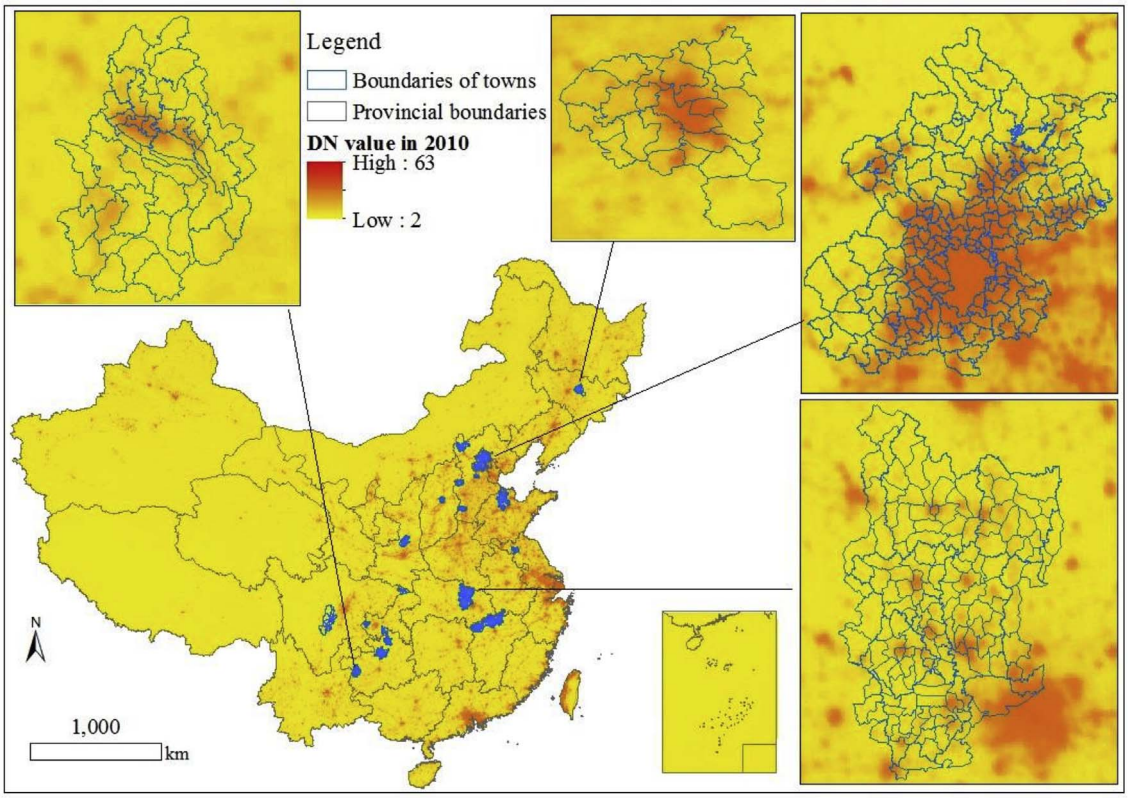

Fig. 4. The distribution of samples (towns/sub-districts) used for model validation in China in 2010.

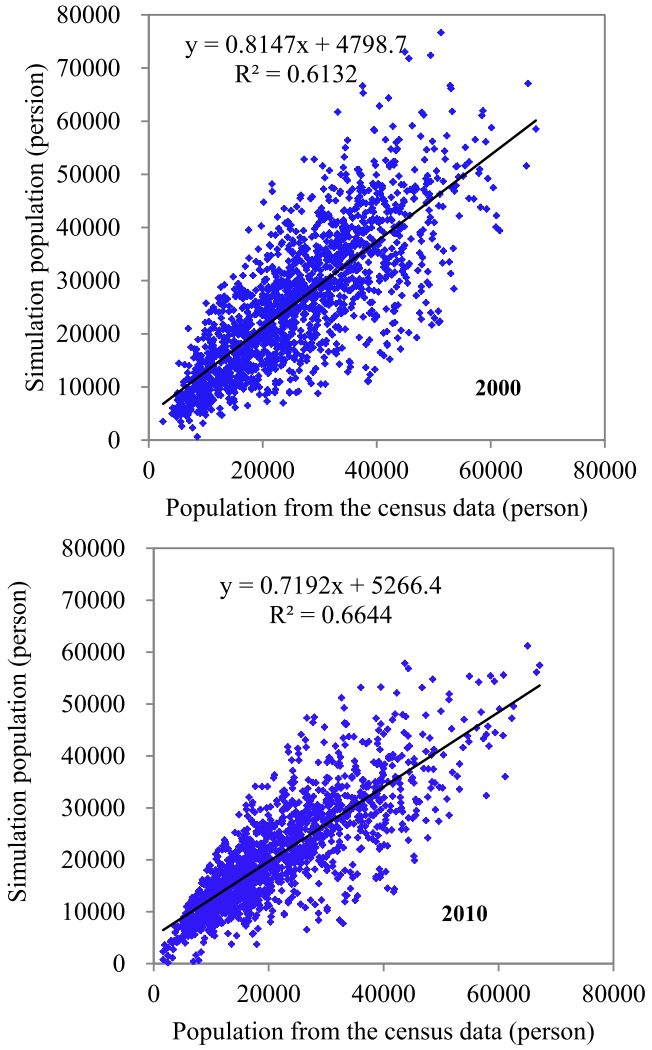

Fig. 5. Comparison of the census data with the model simulation results in 2000 and 2010.

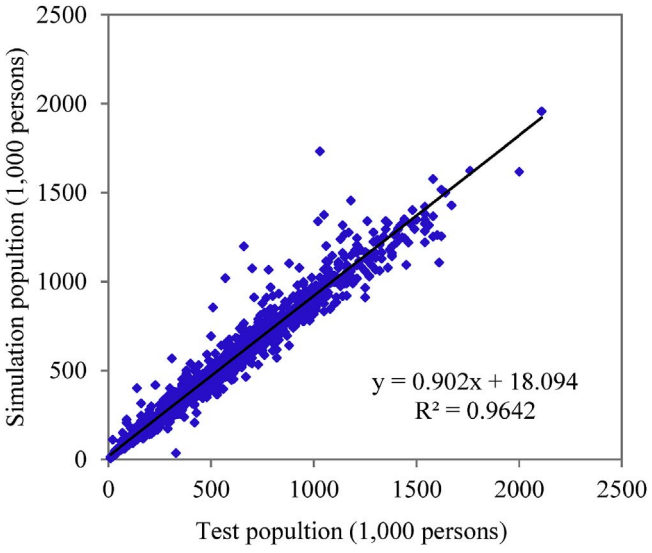

Fig. 6. Comparison of the statistical population (NBSC, 2006) with the model simulation results in 2005.

the data availability.

3. Results and analysis

By using the above method, we obtained the Chinese mainland population density diagrams in 2000 and 2010, with a spatial resolution of 1 × 1 km. Prior to analyzing the research results, we verified the model simulation results. Thus, on the basis of ensuring data accuracy, we carried out further analyses on the population spatial pattern and its variation in the first ten years of the 21st century.

3.1. Model validation results

We used the census data of 1720 towns/sub-districts in 2000 and 1495 towns/sub-districts in 2010 in Jilin Province, Jiangsu Province, Shandong Province, Beijing Municipality, Hebei Province, Shaanxi Province, Shanxi Province, Hubei Province, Jiangxi Province, Sichuan Province, Guizhou Province, and Chongqing Municipality to verify the population simulation data in 2000 and 2010, respectively (Figs. 1 and 4). These towns/sub-districts covered urban areas, suburbs, and rural areas.

The verification results showed that the census data were significantly positively correlated with the simulation data, with determination coefficients (R^2) greater than 0.6 (Fig. 5). This proved that the method can adequately simulate the spatial distribution of populations, using land use data, nighttime light imagery, and census data. As mentioned in the Introduction (Table 1), previous studies also used spatialized population density maps, based on variables in terms of land use data, nighttime light imagery, roads, railways, elevation, soil, etc. However, these methods are often time- and labor-consuming (Zeng et al., 2011).

In addition, most studies compare modeled results with census data at the county level to verify the accuracy of the results. In this study, the calculated total population has been calibrated by the census data at the county level using Eq. (5). For a county, its modeled total population equaled its census data; it is therefore not necessary to verify model results at the country level. Thus, we used the census data of the sub-county level (town) to test the model results, which is often ignored in previous studies.

In Non-census years, it is very difficult to obtain population data at the sub-county level (town). This study tested the model results using the statistical population data at the county level in 2005. The test result showed that the statistical data were significantly positively correlated with the simulation data, and determination coefficients (R^2) was 0.902 (NBSC, 2006) (Fig. 6). This proved that the method can adequately simulate the spatial distribution of populations in non-census years.

3.2. Spatial distribution pattern of population in China

Studying population spatial distribution always involves the spatial classification problem of population density. According to the fifth census, if the population density of a municipal district was more than 1500 persons/km^2, the entire population was included in the urban population. On this basis, this paper regarded the pattern spots with population density more than 1500 persons/km^2 as high population density regions (Fig. 7). In addition, for the convenience of carrying out comparisons with previous research, hierarchical classification also referred to the existing classification methods (Tian et al., 2005).

From 2000 to 2010, the regions (grids) with population density between 200 and 1500 persons/km^2 showed a feature of significant reduction, especially the regions with population density between 500 and 1500 persons/km^2, whose area decreased by 41% from 589,000 km^2 in 2000 to 346,000 km^2 in 2010 (Table 2). These regions are located in the plains of Henan Province, Shandong Province, Hebei Province, and Sichuan Province, which are China's major grain-

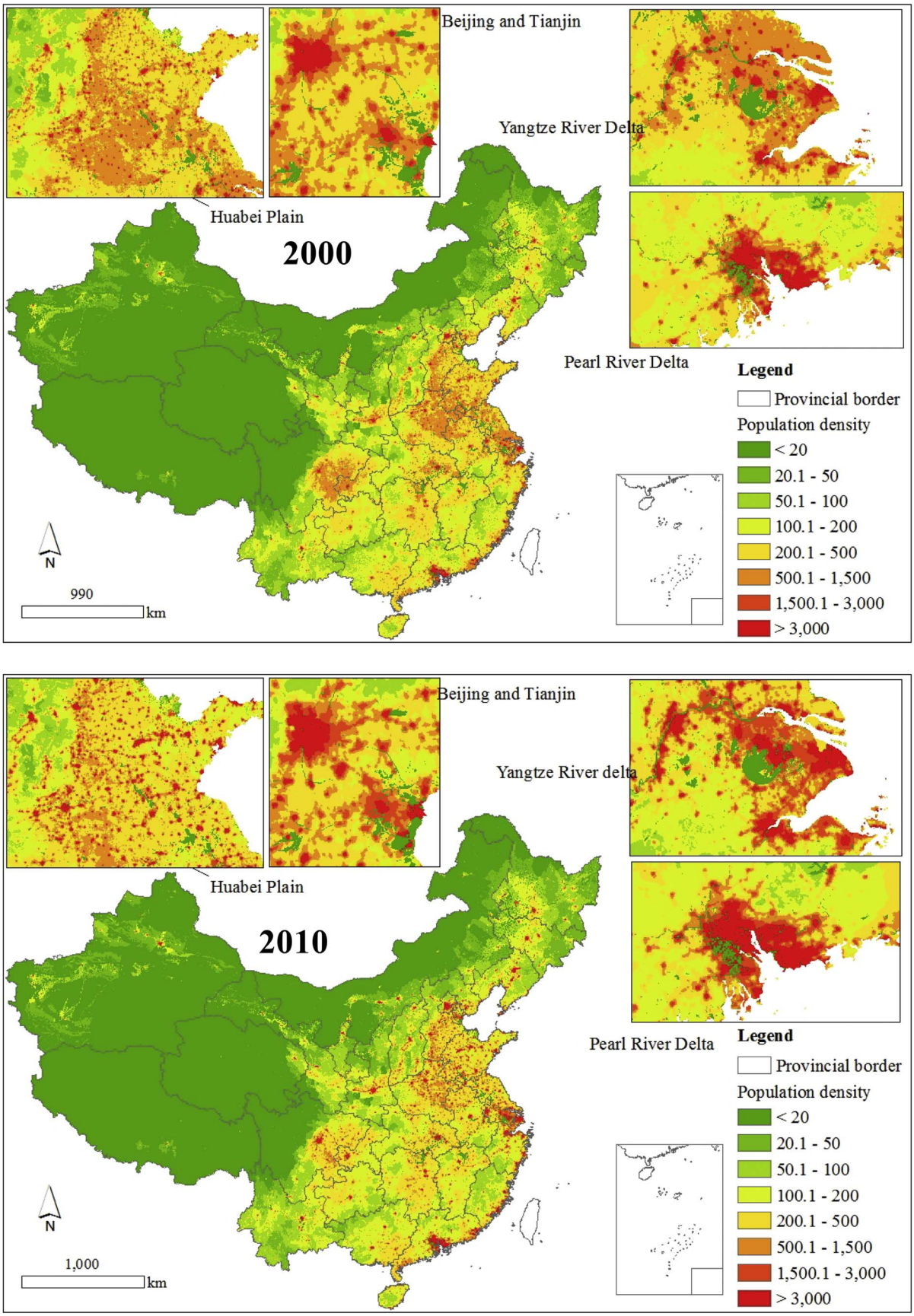

Fig. 7. Simulated population density (persons/km^2) in China in 2000 and 2010.

Table 2
Changes in population densities in the 2010s.

Regional division	Regional type	Population density	Land area in 2000	Land area in 2010	Population in 2000	Population in 2010
		(persons/km^2)	(10^3 km^2)	(10^3 km^2)	(10^6 person)	(10^6 person)
Low-density regions	1	< 20	5231	5170	13.2	14.5
	2	20.1–50	739	889	26.1	30.7
	3	50.1–100	1015	1124	73.9	82.0
	4	100.1–200	876	896	124.9	127.2
Intermediate-density regions	5	200.1–500	921	889	300.2	283.8
	6	500.1–1500	586	345	433.9	267.7
High-density regions	7	1500.1–3000	31	75	64.0	158.7
	8	> 3000	31	66	182.6	352.8

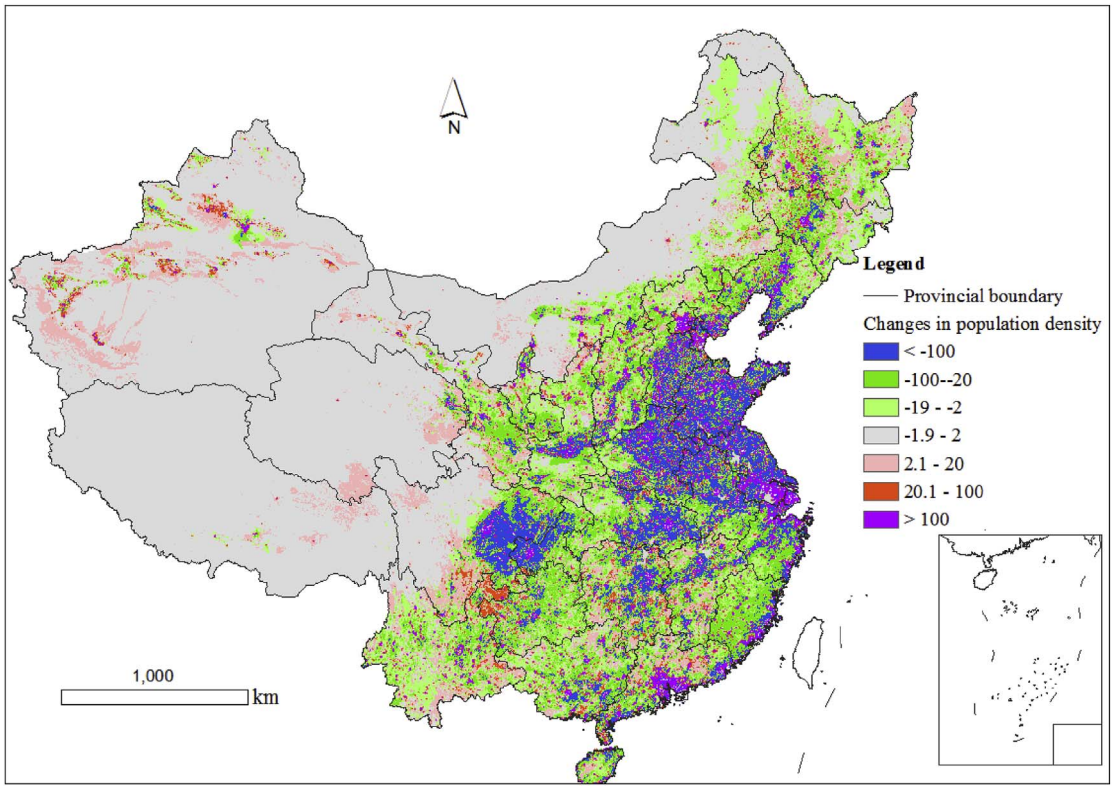

Fig. 8. Variation of Chinese population density during the period 2000–2010 (persons/km^2).

producing areas. In the intermediate-density regions, the amplitude of population reduction in many districts was more than 100 persons/km^2 (Table 2 and Fig. 8). In the future, with the continuing implementation of the urbanization process, the “disappearance” phenomenon of intermediate-density regions will become more common. At present, the farmers of China are generally more than 50 years old. With the improvement of the agricultural mechanization level and the evolution of the rural population age structure, the large-scale operation of agriculture is inevitable in the future. However, the population density of these regions is still very high. For the regions with a population density between 200 and 500 persons/km^2, the land area per capita is between 2000 and 5000 m^2, and the cultivated land area per capita is even lower.

Table 2 shows that from 2000 to 2010, the area of the regions with population density more than 3000 persons/km^2 expanded by 112% from 31,000 km^2 to 66,000 km^2. Accordingly, the population of these regions increased by 93%. By 2010, the regions had a total population of about 350 million. Similarly, the area of the regions with population density between 1500 and 3000 persons/km^2 also presented a substantial increase by 142%, and the population increased by 148%. The average population density of these regions showed a slight increase.

The area of the regions with a population density less than 200 persons/km^2 also showed an expansion tendency, which increased by about 200,000 km^2 from 7.89 million km^2 in 2000 to 8.09 million km^2 in 2010 (Table 2). The spatial growth of low-density regions was mainly a result of the population decline of intermediate-density regions. In addition, the population decline tendency inside the low-density regions was also very clear. For example, the population density in mountainous areas of China's southeastern coastal areas and provincial administrative units such as Guizhou, Sichuan, and Chongqing markedly decreased. This population density decline greatly decreased land use intensity, which alleviated the ecological pressure (Hao, Li, Zhang, Zhang, & Tan, 2015).

4. Conclusions

Based on land use map, census data, and light image, this paper carried out spatial matching on the population of each county, simulated the spatial distribution and its variation of Chinese population in the first decade of this century, and developed population density diagrams for 2000 and 2010. The proposed method was relatively simple. The simulation results were verified by the census data at the

township level. The main conclusions can be drawn as follows:

1) The results showed that the census data had a significant linear positive correlation with the simulation data at the township/sub-district level, with a determination coefficient (R^2) greater than 0.6, which implied that the model provided in this study had a high simulation precision.
2) High-density regions presented a trend of rapid growth. From 2000 to 2010, the area of regions with a population density of more than 3000 persons/km^2 increased by 112% from 31,000 km^2 to 66,000 km^2, with a population increase of 93% accordingly.
3) From 2000 to 2010, we observed a "disappearance" phenomenon of intermediate-density regions. The regions with a population density between 200 and 1500 persons/km^2 showed a significant decrease.

The expansion of high- and low-density regions and the "disappearance" of intermediate-density regions exert a significant impact on the spatial distribution of anthropogenic pressure on natural environments in China.

Acknowledgments

This work was supported by the Natural Science Foundation of China (Grant No. 41771116), the National Basic Research Program of China (Grant No. 2015CB452705); and National Key Research and Development Program of China (Grant No: 2016YFC0502103).

Appendix A. Supplementary data

Supplementary data related to this article can be found at http://dx.doi.org/10.1016/j.apgeog.2017.12.012.

References

Amaral, S., Câmara, G., Monteiro, A. M. V., Quintanilha, J. A., & Elvidge, C. D. (2005). Estimating population and energy consumption in Brazilian Amazonia using DMSP night-time satellite data. *Computers, Environment and Urban Systems, 29*, 179–195.

Anderson, S. J., Tuttle, B. T., Powell, R. L., & Sutton, P. C. (2010). Characterizing relationships between population density and nighttime imagery for denver, Colorado: Issues of scale and representation. *International Journal of Remote Sensing, 31*, 5733–5746.

Bagan, H., & Yamagata, Y. (2015). Analysis of urban growth and estimating population density using satellite images of nighttime lights and land-use and population data. *GIScience and Remote Sensing*. http://dx.doi.org/10.1080/15481603.15482015.11072400.

Chen, X., & Nordhausa, W. D. (2011). Using luminosity data as a proxy for economic statistics. *Proceedings of the National Academy of Sciences, 108*, 8589–8594.

Dobson, J. E., Brlght, E. A., Coleman, P. R., Durfee, R. C., & Worley, B. A. (2000). LandScan: A global population database for estimating populations at risk. *Photogrammetric Engineering & Remote Sensing, 66*, 849–857.

Elvidge, C. D., Imhoff, M. L., Baugh, K. E., Hobson, V. R., Nelson, I., Safran, J., et al. (2001). Night-time lights of the world: 1994-1995. *ISPRS Journal of Photogrammetry and Remote Sensing, 56*, 81–99.

Elvidge, C. D., Sutton, P. C., Ghosh, T., Tuttle, B. T., Baugh, K. E., Bhaduri, B., et al. (2009). A global poverty map derived from satellite data. *Computers & Geosciences, 35*, 1652–1660.

Hao, H., Li, X., Zhang, H., Zhang, J., & Tan, M. (2015). Impact of the opportunity cost of farming labor on the agricultural land marginalization. *Journal of Arid Land Resources and Environment, 29*, 50–56.

Hsu, F. C., Baugh, K. E., Ghosh, T., Zhizhin, M., & Elvidge, C. D. (2015). DMSP-ols radiance calibrated nighttime lights time series with intercalibration. *Remote Sensing, 7*, 1855–1876. http://dx.doi.org/10.3390/rs70201855.

Imhoff, M. L., Lawrence, W. T., Stutter, D. C., & Elvidget, C. D. (1997). A technique for using composite DMSP/OLS"City lights" satellite data to map urban area. *Remote Sensing of Environment, 61*, 361–371.

Keola, S., Andersson, M., & Hall, O. (2015). Monitoring economic development from Space: Using nighttime light and land cover data to measure economic growth. *World Development, 66*, 322–334.

Levin, N., & Duke, Y. (2012). High spatial resolution night-time light images for demographic and socio-economic studies. *Remote Sensing of Environment, 119*, 1–10.

Li, S., Sun, Z., Tan, M., & Li, X. (2016). Effects of rural–urban migration on vegetation greenness in fragile areas: A case study of inner Mongolia in China. *Journal of Geographical Sciences, 26*, 313–324.

Liu, J., Liu, M., Deng, X., Zhuang, D., & Zhang, Z. (2002). The land use and land cover change database and its relative studies in China. *Journal of Geographical Sciences, 12*, 275–282.

Liu, J., Liu, M., & Zhuang, D. (2003a). Study on spatial pattern of land-use change in China during 1995-2000. *Science in China (Series D). Science in China (Series D), 46*, 373–384.

Liu, J., Yue, T., Wang, Y., Qiu, D., Liu, M., Deng, X., et al. (2003b). Digital simulation of population density in China. *Acta Geographica Sinica, 58*, 17–24.

Lo, C. P. (2001). Modeling the population of China using DMSP operational linescan System nighttime data. *Photogranimetric Engintering and Rrmote Sensing, 67*, 1037–1047.

Lung, T., Lübker, T., Ngochoch, J. K., & Schaab, G. (2013). Human population distribution modelling at regional level using very high resolution satellite imagery. *Applied Geography, 41*, 36–45.

Lu, D., Tian, H., Zhou, G., & Ge, H. (2008). Regional mapping of human settlements in southeastern China with multisensor remotely sensed data. *Remote Sensing of Environment, 112*, 3668–3679.

Ma, T., Zhou, Y., Zhou, C., Haynie, S., Pei, T., & Xu, T. (2015). Night-time light derived estimation of spatio-temporal characteristics of urbanization dynamics using DMSP/OLS satellite data. *Remote Sensing of Environment, 158*, 453–464.

National Bureau of Statistics of China (NBSC) (2013). *China city statistical Yearbook*. Beijing: China Statistic Press.

National Bureau of Statistics of China (NBSC) (2002). *Tabulation on the 2000 population census of the People's Republic of China*. Beijing: China Statistics Press.

National Bureau of Statistics of China (NBSC) (2006). *China county statistical Yearbook in 2006*. Beijing: China Statistics Press.

National Bureau of Statistics of China (NBSC) (2012). *Tabulation on the 2010 population census of the People's Republic of China*. Beijing: China Statistics Press.

Pandey, B., Joshi, P. K., & Seto, K. C. (2013). Monitoring urbanization dynamics in India using DMSP/OLS night time lights and SPOT-VGT data. *International Journal of Applied Earth Observation and Geoinformation, 23*, 49–61.

Propastin, P., & Kappas, M. (2012). Assessing satellite-observed nighttime lights for monitoring socioeconomic parameters in the Republic of Kazakhstan. *GIScience and Remote Sensing, 49*, 538–557.

Ryan, S. J., Palace, M. W., Hartter, J., Diem, J. E., Chapman, C. A., & Southworth, J. (2017). Population pressure and global markets drive a decade of forest cover change in Africa's Albertine Rift. *Applied Geography, 81*, 52–59.

Saksena, S., Fox, J., Spencer, J., Castrence, M., DiGregorio, M., Epprecht, M., et al. (2014). Classifying and mapping the urban transition in Vietnam. *Applied Geography, 50*, 80–89.

Shao, Z., & Liu, C. (2014). The integrated use of DMSP-OLS nighttime light and MODIS data for monitoring large-scale impervious surface dynamics: A case study in the Yangtze river delta. *Remote Sensing, 6*, 9359–9378 doi:9310.3390/rs6109359.

Small, C., Pozzi, F., & Elvidge, C. D. (2005). Spatial analysis of global urban extent from DMSP-OLS night lights. *Remote Sensing of Environment, 96*, 277–291.

Su, Y., Chen, X., Wang, C., Zhang, H., Liao, J., Ye, Y., et al. (2015). A new method for extracting built-up urban areas using DMSP-OLS nighttime stable lights: A case study in the Pearl river delta, southern China. *GIScience and Remote Sensing, 52*, 218–238.

Sutton, P. (1997). Modeling population density with night-time stallite imagery and GIS. *Computers, Environment and Urban Systems, 21*, 227–244.

Tan, M. (2015). Urban growth and rural transition in China based on DMSP/OLS night-time light data. *Sustainability, 7*, 8768–8781.

Tan, M., Li, X., Lu, C., Luo, W., Kong, X., & Ma, S. (2008). Urban population densities and their policy implications in China. *Habitat International, 32*, 471–484.

Tian, Y., Yue, T., Zhu, L., & Clinton, N. (2005). Modeling population density using land cover data. *Ecological Modelling, 189*, 72–88.

Tritsch, I., & Le Tourneau, F. (2016). Population densities and deforestation in the Brazilian Amazon: New insights on the current human settlement patterns. *Applied Geography, 76*, 163–172.

Wang, L., Feng, Z., Yang, Y., & You, Z. (2014). The change of population density and its influencing factors from 2000 to 2010 in China on county scale. *Acta Geographica Sinica, 69*, 1790–1798.

Wei, Y., Liu, H., Song, W., Yu, B., & Xiu, C. (2014). Normalization of time series DMSP-OLS nighttime light images for urban growth analysis with Pseudo Invariant Features. *Landscape and Urban Planning, 128*, 1–13.

Wu, J., Wang, Z., Li, W., & Peng, J. (2013). Exploring factors affecting the relationship between light consumption and GDP based on DMSP/OLS nighttime satellite imagery. *Remote Sensing of Environment, 134*, 111–119.

Xiao, P., Wang, X., Feng, X., Zhang, X., & Yang, Y. (2014). Detecting China's urban expansion over the past three decades using nighttime light data. *IEEE Journal of Selected Topics in Applied Earth Observations and Remote Sensing, 7*(10), 1–12.

Yang, X., Jiang, G., Luo, X., & Zheng, Z. (2012). Preliminary mapping of high-resolution rural population distribution based on imagery from Google earth: A case study in the lake tai basin, eastern China. *Applied Geography, 32*, 221–227.

Yi, K., Tani, H., Li, Q., Zhang, J., Guo, M., Bao, Y., et al. (2014). Mapping and evaluating the urbanization process in northeast China using DMSP/OLS nighttime light data. *Sensors, 14*, 3207–3226 doi:3210.3390/s140203207.

Yue, W., Zhang, L., & Liu, Y. (2016). Measuring sprawl in large Chinese cities along the Yangtze River via combined single and multidimensional metrics. *Habitat International, 57*, 43–52.

Zeng, C., Zhou, Y., Wang, S., Yan, F., & Zhao, Q. (2011). Population spatialization in China based on night-time imagery and land use data. *International Journal of Remote Sensing, 32*, 9599–9620.

Zhang, K. H., & Song, S. (2003). Rural–urban migration and urbanization in China: Evidence from time-series and cross-section analyses. *China Economic Review, 14*, 386–400.

Zhang, Q., & Su, S. (2016). Determinants of urban expansion and their relative importance: A comparative analysis of 30 major metropolitans in China. *Habitat*

International, 58, 89–107.
Zhou, Y., Smith, S. J., Elvidge, C. D., Zhao, K., Thomson, A., & Imhoff, M. (2014). A cluster-based method to map urban area from DMSP/OLS nigh tlights. *Remote Sensing of Environment, 147*, 173–185.
Zhuo, L., Chen, J., Shi, P., Gu, Z., Fan, Y., & Toshiaki, I. (2005). Modeling population density of China in 1998 based on DMSP/OLS nighttime light image. *Acta Geographica Sinica, 60*, 266–276.